*Article*

# Extracting the DBH of Moso Bamboo Forests Using LiDAR: Parameter Optimization and Accuracy Evaluation

**Longwei Li [1,2,3,†], Linjia Wei [1,†], Nan Li [2,3,*], Shijun Zhang [1], Zhicheng Wu [2], Miaofei Dong [2] and Yuyun Chen [4]**

[1]   School of Resources and Environmental Engineering, Anhui University, Hefei 230601, China;
    lilw@chzu.edu.cn (L.L.); x22301048@stu.ahu.edu.cn (L.W.); x23301161@stu.ahu.edu.cn (S.Z.)
[2]   School of Geographic Information and Tourism, Chuzhou University, Chuzhou 239000, China;
    2021210074@mail.chzu.edu.cn (Z.W.); 2021210113@mail.chzu.edu.cn (M.D.)
[3]   Anhui Province Key Laboratory of Physical Geographic Environment, Chuzhou 239000, China
[4]   Shanghai Ubiquitous Navigation Technology Co., Ltd., Shanghai 201799, China; chenyuyun@ubinavi.com.cn
[*]   Correspondence: linan@chzu.edu.cn
[†]   These authors contributed equally to this work.

**Abstract:** The accurate determination of the Diameter at Breast Height (DBH) of Moso bamboo is crucial for estimating biomass and carbon storage in Moso bamboo forests. In this research, we utilized handheld LiDAR point cloud data to extract the DBH of Moso bamboo and enhanced the accuracy of diameter fitting by optimizing denoising parameters. Specifically, we fine-tuned two denoising parameters, neighborhood point number and standard deviation multiplier, across five gradient levels for denoising. Subsequently, DBH fitting was conducted on data processed with varying denoising parameters, followed by a precision evaluation to investigate the key factors influencing the accuracy of Moso bamboo DBH fitting. The research results indicate that a handheld laser was used to scan six plots, from which 132 single Moso bamboo trees were selected. Out of these, 122 single trees were successfully segmented and identified, achieving an accuracy rate of 92.4% in identifying single Moso bamboo trees, with an average accuracy of 95.64% in extracting DBH for individual plants; the mean error was ±1.8 cm. Notably, setting the minimum neighborhood point to 10 resulted in the highest fitting accuracy for DBH. Moreover, the optimal standard deviation multiplier threshold was found to be 1 in high-density forest plots and 2 in low-density forest plots. Forest condition and slope were identified as the primary factors impacting the accuracy of Moso bamboo DBH fitting.

**Keywords:** Moso bamboo; handheld LiDAR; individual tree detection; DBH; error analysis

## 1. Introduction

Moso bamboo (*Phyllostachys edulis*) is an evergreen plant that is commonly found in tropical and subtropical regions [1]. It holds significant economic importance in China due to its widespread distribution [2–4]. The edible bamboo shoots and versatile material properties of Moso bamboo make it highly valuable [5]. The extensive root system of Moso bamboo plays a crucial ecological role in windbreaks, sand stabilization, water conservation, and soil preservation [6]. Moso bamboo exhibits rapid growth, achieving maturity within a short span of 50 to 60 days from the emergence of shoots [7]. Its distinctive mechanism of biomass accumulation highlights its substantial potential for carbon sequestration, making a significant contribution to the global carbon sink [8,9].

Accurately estimating the individual parameters of Moso bamboo is crucial for determining its carbon storage capacity. Forestry researchers evaluate tree health by monitoring the growth of individual trees in a forest, often using quantitative indicators like DBH to ensure consistency in forest inventory results [10]. Laser scanning technology employs a laser emitter to emit pulsed laser beams and scan the surrounding environment, collecting precise three-dimensional point cloud data by measuring distances to target surfaces. This

process effectively captures detailed spatial information, including the shape, size, and depth of objects in a scanned area. [11]. This technology is particularly adept at extracting individual tree parameters for forestry applications [12]. Polewski et al. (2019) introduced an algorithm for matching unmarked airborne laser scanning (ALS) and backpack LiDAR data, enhancing the measurement of forest resources through unmarked data matching [13]. Cai et al. (2021) enhanced DBH fitting accuracy by filtering out noise points with varying intensities in point cloud data [14]. Brolly et al. (2021) utilized LiDAR technology to estimate individual tree structural parameters by creating digital terrain models (DTMs), tree canopy surface models, and trunk models to derive stand parameters [15]. Cai et al. (2018) developed a method to rapidly determine bamboo age by analyzing the relationship between point cloud data echo intensity and bamboo age, achieving an accuracy of 92.5% [16]. Li et al. (2022) conducted a study comparing crown heights measured from individual trees in sample sites with those extracted from LiDAR point cloud data, resulting in a Root Mean Square Error (*RMSE*) of 1.33 m and a coefficient of determination ($R^2$) of 0.96 [17].

Several studies have utilized Terrestrial Laser Scanning (TLS) data to analyze the extraction of DBH in Moso bamboo. Huang et al. (2021) employed TLS technology to capture point cloud data from Moso bamboo forest locations [18]. By conducting a thorough examination of bamboo stem shapes and forest conditions, they introduced a novel stem recognition method that enhanced the identification rate of individual Moso bamboo plants in point cloud data and the accuracy of DBH estimation. Similarly, Jiang et al. (2022) conducted TLS multi-station scanning to gather point cloud data from Moso bamboo forests [19]. By fitting a circular cross-section of bamboo stems and establishing a longitudinal axis of bamboo stems, they derived the DBH and pole length of Moso bamboo, minimizing parameter errors caused by bamboo pole bending. These studies primarily focus on enhancing the accuracy of DBH estimation by investigating the influence of Moso bamboo's growth structure. Additionally, the quality of point cloud data significantly impacts the accuracy of DBH estimation in Moso bamboo. Noise points within the data are identified as a key factor affecting the quality of point cloud data [20].

This study investigates the factors influencing the denoising of point cloud data, focusing on two main questions: (1) How does the fitting accuracy of Moso bamboo DBH change under various denoising parameter conditions? (2) What are the optimal denoising parameters? The analysis in this paper aims to identify the sources of errors and offer insights for parameter extraction for individual Moso bamboo using handheld LiDAR technology.

## 2. Materials and Methods

### 2.1. Study Area

The study area is situated in the Taipinghu and Wushi Towns, Huangshan City, in the southern region of Anhui Province, China (Figure 1a–c). This area experiences a subtropical humid monsoon climate, with an average annual rainfall of 1274.7 mm, 1711.0 h of sunshine per year, and an average annual temperature of 16.6 °C in 2022 (Huangshan Statistical Bureau, 2023, Huangshan, China). The study area is rich in forest resources and benefits from favorable climate conditions that promote vegetation growth. Notable tree species present include *Phyllostachys edulis*, *Cunninghamia lanceolata*, *Pinus massoniana*, and *Liquidambar formosana*, among others (Huangshan Forestry Bureau, 2021, Huangshan, China).

### 2.2. Data Collection

#### 2.2.1. Field Data

Six sample sites of Moso bamboo forests were selected in the study area (Figure 1c), each measuring 20 m × 20 m (Figure 2a). Basic information on the sample sites can be found in Table 1. Trees with DBH greater than 5 cm were individually tagged and measured using a diameter ruler, with species category information recorded. Additionally, the coordinates of the center point and four corners of each sample were obtained using the Real-Time

Kinematic (RTK) technique of the Global Navigation Satellite System (GNSS) receiver for later matching with the results of individual tree segmentation.
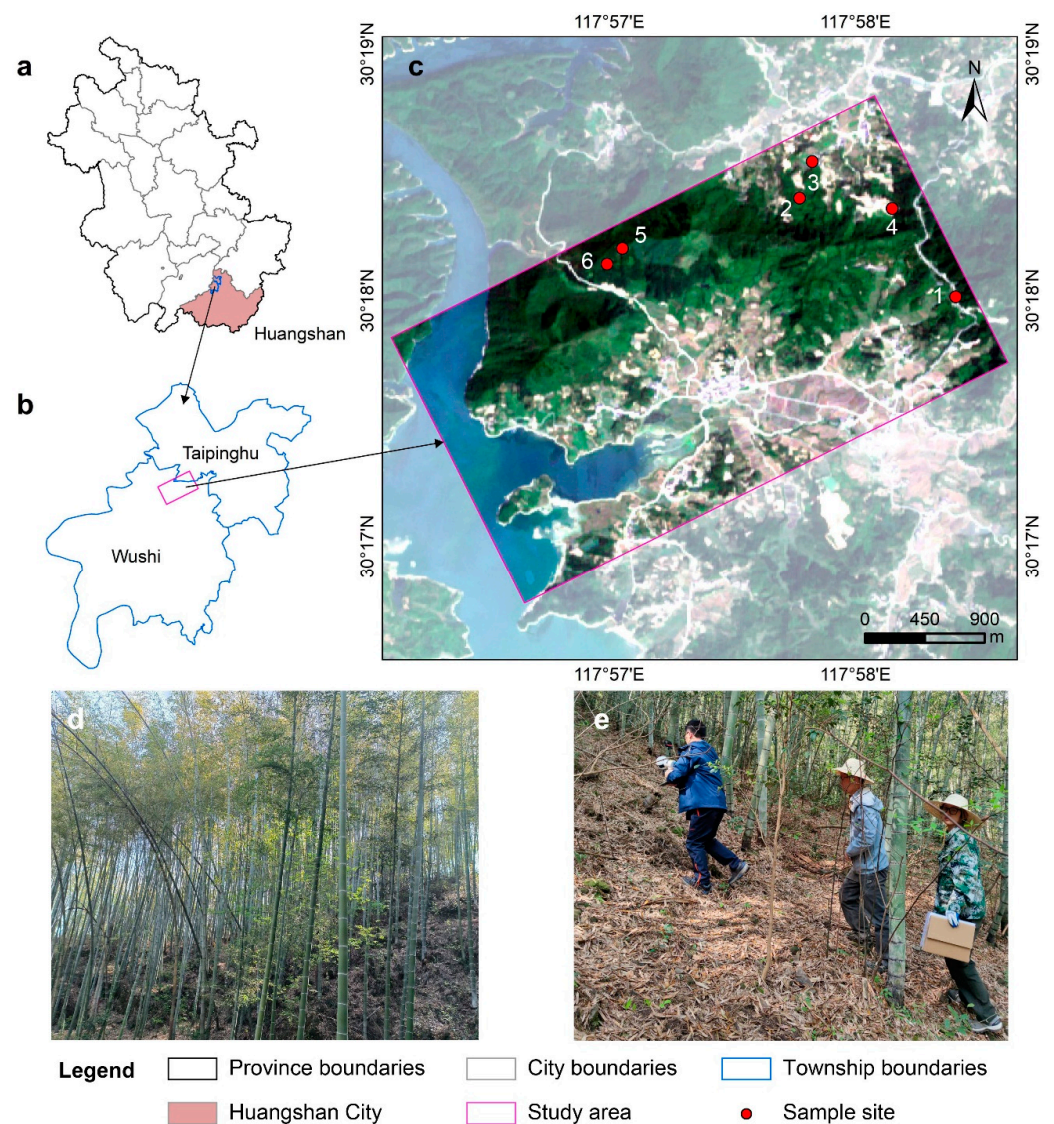


**Figure 1.** Study area. (**a**) Anhui Province, China. (**b**) Taipinghu and Wushi townships in Huangshan City. (**c**) Sample sites. (**d**) Forest condition map of site 3. (**e**) Collecting point cloud data using LiGrip-V100.

**Table 1.** Summary of sample site information for Moso bamboo forest.

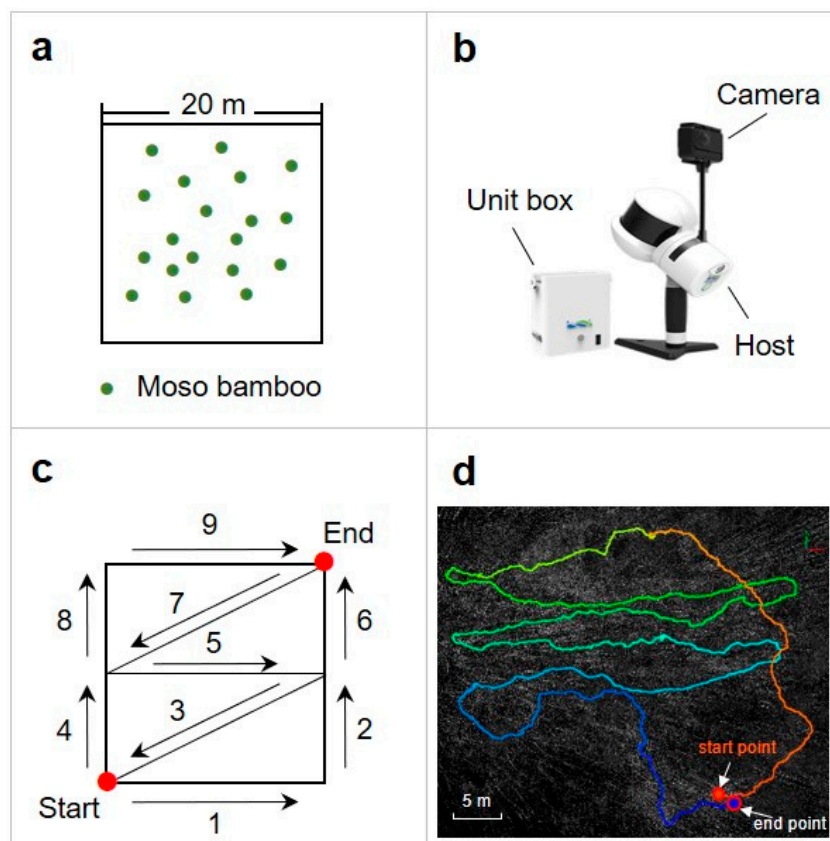| Serial Number | Sample Size | Number of Plants | Under-Forest Condition | Average Slope |
|---|---|---|---|---|
| Site 1 | 20 m × 20 m | 27 | Few shrubs | 5° |
| Site 2 | 20 m × 20 m | 18 | Shrubby | 9° |
| Site 3 | 20 m × 20 m | 27 | Shrubby | 13° |
| Site 4 | 20 m × 20 m | 20 | Shrubby | 25° |
| Site 5 | 20 m × 20 m | 20 | Few shrubs | 15° |
| Site 6 | 20 m × 20 m | 20 | Few shrubs | 5° |

**Figure 2.** Sample site information. (**a**) Schematic diagram of sample site. (**b**) LiGrip-V100 handheld rotary laser scanner. (**c**) Z–shaped route. (**d**) Scanning trajectory.

### 2.2.2. Handheld LiDAR Data

The handheld LiDAR equipment was Green Valley International's model, the LiGrip-V100 handheld rotary laser scanner (Green Valley, Bejing, China), with specifications shown in Table 2. Given the dense Moso bamboo forest terrain with a certain slope, a LiGrip-V100 handheld rotary laser scanner was employed with a double Z–shaped route to optimize point cloud data acquisition (Figure 2b,c). To maintain data quality, a constant scanning speed was maintained while ensuring equipment stability to prevent rotational movements. The walking speed was maintained between 0.8 and 1.2 m/s depending on the terrain. The cloud profiles of the sample site are illustrated in Figure 3.

**Table 2.** Handheld LiDAR parameters.

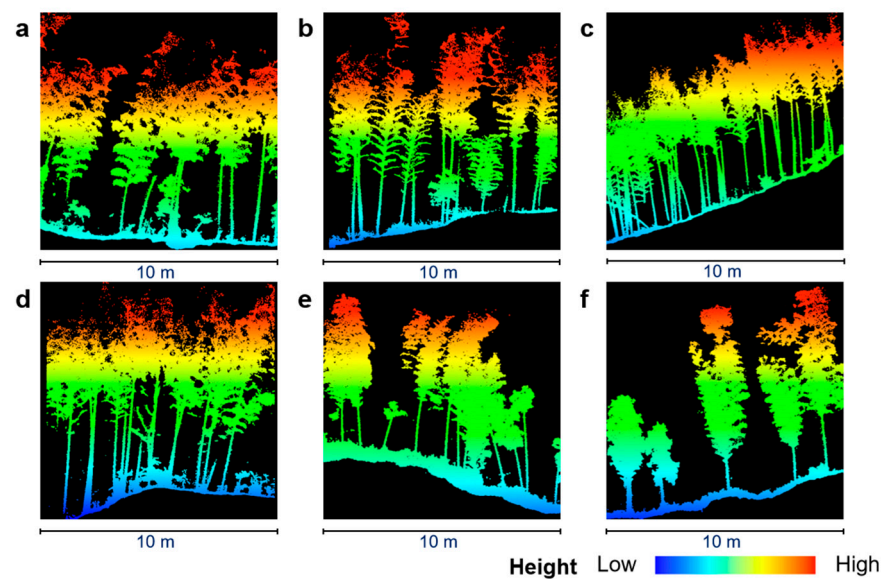| Performance Indicators | Parameters |
| --- | --- |
| Laser Sensor | VLP–16 |
| LiDAR Accuracy | $\pm3$ cm |
| Relative Accuracy | $\leq3$ cm |
| Absolute Accuracy | 5 cm |
| Size | L270 mm $\times$ W210 mm $\times$ H120 mm |
| Laser Wavelength | 903 nm |
| Scan Rate | 300000 pts/s |
| View Angle Range | 280°~360° (Horizontal); –90°~90° (Vertical) |
| Scan Range | 100 m |

**Figure 3.** Sample site cloud profiles. (**a**–**f**) refer to sample sites 1–6, respectively.

*2.3. Moso Bamboo DBH Extraction Methods*

The process of extracting the DBH of Moso bamboo included denoising, ground point classification, point cloud normalization, individual tree segmentation, extraction of single tree DBH, accuracy verification, and denoising parameter optimization (Figure 4).
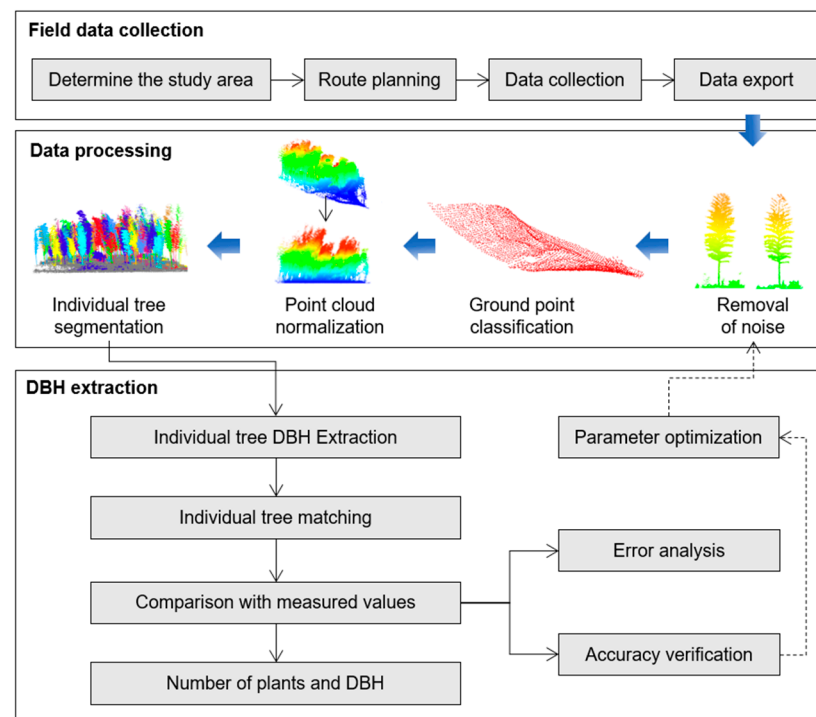


**Figure 4.** Framework for Moso bamboo DBH extraction.

2.3.1. Removal of Noise

The handheld LiDAR data was processed using LiDAR360 V7.0 software (Green Valley, Beijing, China). Initially, the point cloud data underwent cropping based on the sample extent and filtering to remove redundancy and noise (Figure 5). Statistical filtering was used for denoising in this study. The principle was to search for a specified number of neighboring points for each point, calculating the mean of the distances from each point

to its neighbors. The median and standard deviation of these distance means were then calculated. Points whose mean distance was greater than the maximum distance (maximum distance = median + number of standard deviations × standard deviation) were identified as noise and excluded [21]. The parameters impacting the denoising outcome included the number of neighboring points and the number of standard deviations.
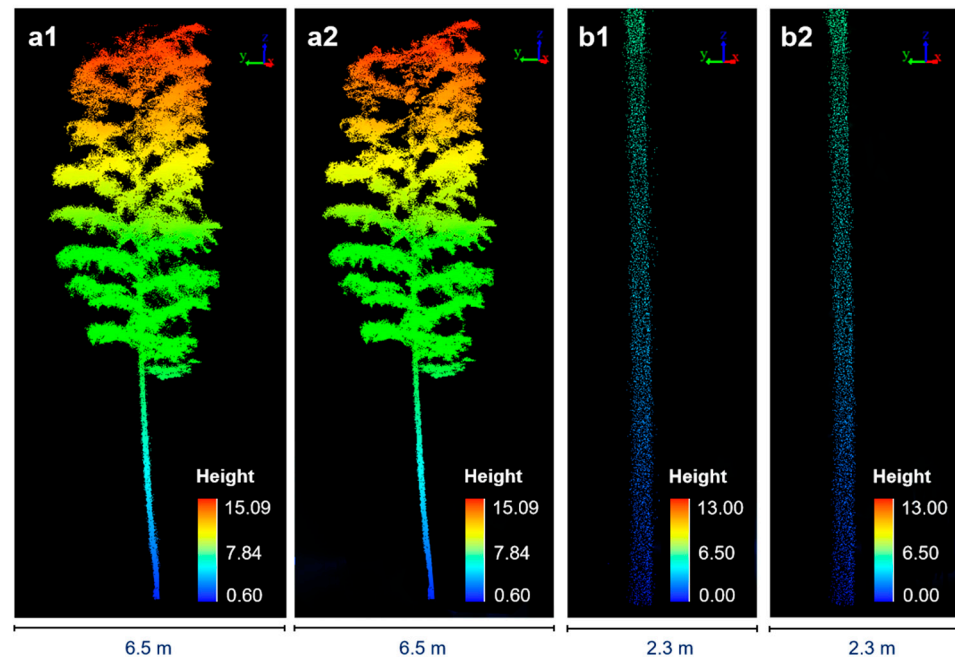


**Figure 5.** Removal of noise. (**a1**,**a2**) are whole plant of Moso bamboo; (**b1**,**b2**) are trunk of Moso Bamboo; (**a1**,**b1**) are point clouds before denoising; (**a2**,**b2**) are point clouds after denoising.

2.3.2. Ground Point Classification and Normalization

The improved progressive triangulated irregular network densification algorithm was applied for ground point classification to mitigate the impact of terrain factors on individual tree segmentation and DBH extraction. The main process consisted of point cloud gridding, selecting seed points, constructing a triangulated irregular network (TIN) using the seed points, and iteratively densifying the TIN. A digital elevation model (DEM) with a resolution of 0.5 m was generated through irregular triangular mesh interpolation [22]. Normalized point cloud data were obtained by subtracting the absolute elevation $Z$ values of the data from the ground points' elevation to eliminate topography influence on tree height estimation [23] (Figure 6).
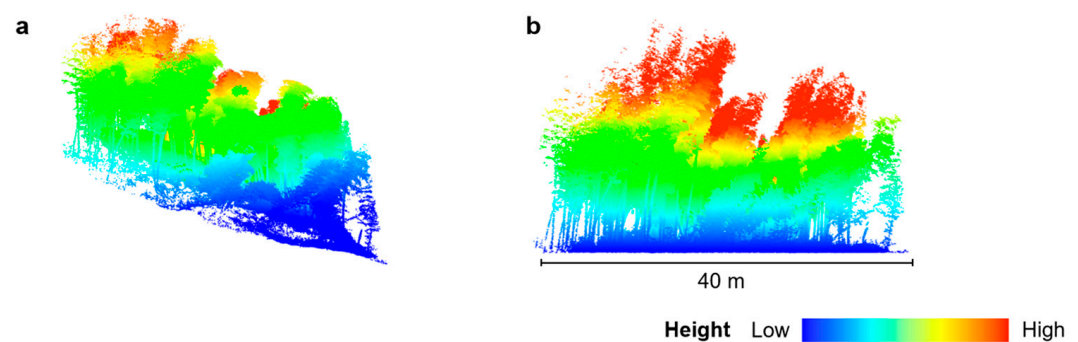


**Figure 6.** Point cloud data normalization. (**a**) Before normalization. (**b**) After normalization.

### 2.3.3. Individual Tree Segmentation

The point cloud segmentation algorithm was utilized for individual tree segmentation [24]. This methodology was based on the spatial separation characteristics between tree canopies. Initially, local maxima detection was performed on the discrete point cloud, assuming that these local highest points represented the treetop. Using this point as a seed point, the point cloud was segmented using a region-growing algorithm. This process was iterated until all significant trees were segmented (Figure 7).
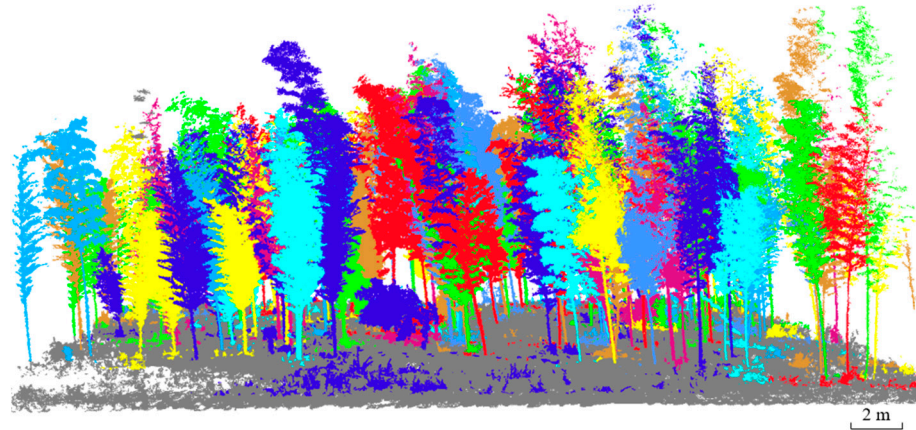


**Figure 7.** Individual tree segmentation result, adjacent trees are distinguished by different colors.

### 2.3.4. DBH Extraction

The DBH of bamboo was extracted using the method of least squares circle fitting. This method achieves the optimal circle center and radius by minimizing the squared error of the sum of distances from all data points to the circumference [25]. In this study, the point cloud of the trunk at 1.3 m above ground was selected for circle fitting (Figure 8).

$$f(x_a, y_a, R) = \sum d_i^2 \tag{1}$$

$$r_i = \sqrt{(x_i - x_a)^2 + (y_i - y_a)^2} \tag{2}$$

where $d_i$ is the distance of each point from the center of the fitted circle at 1.3 m ($d_i = r_i - R$), $x_a$ and $y_a$ are the coordinates of the center of the determined fitted circle, $x_i$ and $y_i$ are the coordinates of the center of the iteratively fitted circle, $r_i$ is the radius of the circle fitted at different points, and $R$ is the radius of the determined fitted circle.
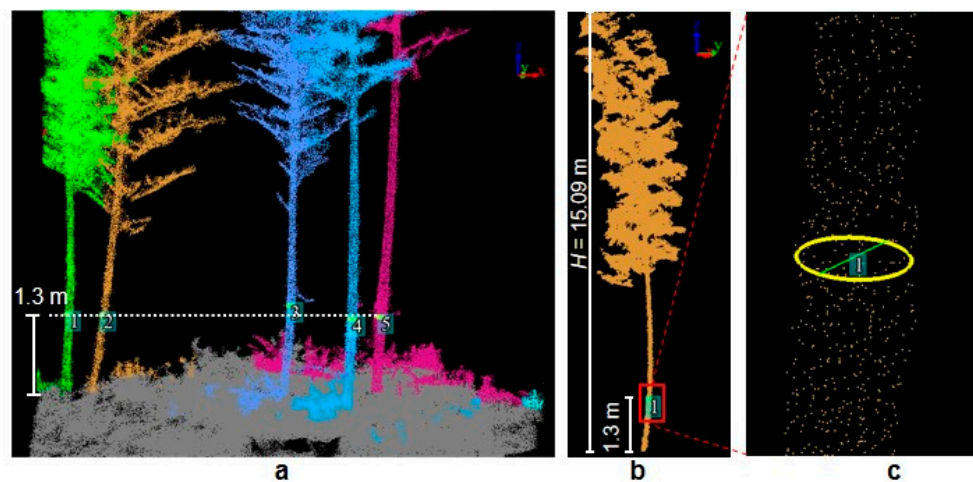


**Figure 8.** Extraction of DBH. (**a**,**b**) DBH fitting height. (**c**) is the partial enlargement of the red square and the yellow circle is the fitted circle.

2.3.5. Denoising Parameter Optimization

In order to identify the best denoising parameters for the point cloud data of a Moso bamboo forest, this study initially set the standard deviation multiplier at 5. Subsequently, varying numbers of minimum neighborhood points (10, 20, 30, 40, 50) were tested for denoising. The DBH was then fitted, and metrics such as precision (*P*), coefficient of determination ($R^2$), *RMSE*, and relative Root Mean Square Error (*rRMSE*) were calculated to compare the fitted values with the measured values. This analysis aimed to determine the optimal parameters for the minimum neighborhood point. Following this, using the identified optimal parameters, the standard deviation multiplier was adjusted to 1, 2, 3, 4, and 5 for further denoising processes. The DBH was fitted once again, and a comparison was made with the measured values to ascertain the most suitable denoising parameters.

2.3.6. Accuracy Assessment

According to the measured RTK coordinates of the Moso bamboo and the point cloud coordinates, a correspondence was established between the measured DBH and the fitted DBH for accuracy verification. This study utilized *P*, $R^2$, *RMSE*, and *rRMSE* to assess the accuracy. A higher $R^2$ indicated a stronger correlation between the measured and fitted values, while a lower *RMSE* signified greater predictive value. The formula is as follows:

$$P = 1 - \frac{1}{n}\sum_{i=1}^{n}\frac{|W_i - w_i|}{W_i} \tag{3}$$

$$R^2 = \frac{\sum_{i=1}^{n}(w_i - \overline{w_i})(W_i - \overline{W_i})}{\sqrt{\sum_{i=1}^{n}(w_i - \overline{w_i})^2 \sum_{i=1}^{n}(W_i - \overline{W_i})^2}} \tag{4}$$

$$RMSE = \sqrt{\frac{1}{n}\sum_{i=1}^{n}(W_i - \overline{W_i})^2} \tag{5}$$

$$rRMSE = \frac{RMSE}{\frac{1}{n}\sum_{i=1}^{n}w_i} \tag{6}$$

where *P* represents precision, $R^2$ represents the coefficient of determination, *RMSE* represents the Root Mean Square Error, *rRMSE* represents the relative Root Mean Square Error, *n* is the number of correctly segregated individual Moso bamboo plants, $W_i$ is the fitted DBH, $w_i$ is the measured DBH, $\overline{W_i}$ is the mean value of $W_i$, and $\overline{w_i}$ is the mean value of $w_i$.

## 3. Results

### 3.1. Identification Results and Analysis of Moso Bamboo

Table 3 displays the number of plants measured, recognized by the handheld LiDAR, and undetected and the detection rate across the six sample sites. The identification accuracy of Moso bamboo varied among the plots, with a 100% identification rate in site 6, 88.89% in sites 1 and 3, and an average of 93% overall. The accuracy of Moso bamboo identification was influenced by factors such as RTK accuracy and the quality of the point cloud data. Site 6 had a sparse distribution of Moso bamboo and fewer understory shrubs, exhibiting high accuracy in single Moso bamboo identification. Conversely, sites 1 and 3 had dense bamboo and poor RTK signals in the understory, resulting in the low identification of single trees.

**Table 3.** Identification results of Moso Bamboo.

| Serial Number | Number of Plants Measured | Number of Plants Identified | Number of Undetected Strains | Recognition Rate (%) |
|---|---|---|---|---|
| Site 1 | 27 | 24 | 3 | 88.89 |
| Site 2 | 18 | 17 | 1 | 94.44 |
| Site 3 | 27 | 24 | 3 | 88.89 |
| Site 4 | 20 | 19 | 1 | 95 |
| Site 5 | 20 | 18 | 2 | 90 |
| Site 6 | 20 | 20 | 0 | 100 |

*3.2. Parameter Optimization Results and Analysis*

The quality of the point cloud data for Moso bamboo forests was enhanced by optimizing denoising parameters prior to fitting the chest diameter. This study investigated the optimal minimum neighborhood point parameter for statistical filtering [26] method to denoise the point cloud data of Moso bamboo forests. Five parameter values were tested for denoising, with a fixed standard deviation multiplier of 5. The extracted DBHs were then compared with the measured values, as shown in Table 4. The results revealed that a minimum neighboring point of 10 yielded the highest accuracy in fitting the cloud DBH of Moso bamboo points in sites 1, 2, 3, 4, and 6, with accuracy rates of 96.37%, 90.44%, 86.80%, 92.39%, and 94.44%, respectively. The $R^2$ values ranged from 0.344 to 0.959, with site 1 achieving the highest fit. The *RMSE* value for site 1 was 0.416, with an *rRMSE* of 4.38%, indicating the best overall fit. Site 5 showed a high accuracy of 90.03% for DBH fit at a minimum neighborhood point of 30, only slightly higher than the accuracy at a minimum neighborhood point of 10. Overall, the most accurate fitting of Moso bamboo diameter was achieved with a minimum neighborhood point of 10, suggesting that noise points could be more precisely removed under this parameter while retaining effective data points that revealed the structure of Moso bamboo.

**Table 4.** DBH fitting results after denoising with different minimum neighborhood point parameters.

| Serial Number | Minimum Number of Neighborhood Points | Accuracy (%) | $R^2$ | RMSE | rRMSE (%) |
|---|---|---|---|---|---|
| Site 1 | 10 | 96.37 | 0.959 | 0.416 | 4.38 |
| | 20 | 94.39 | 0.872 | 0.632 | 6.24 |
| | 30 | 93.87 | 0.906 | 0.700 | 7.36 |
| | 40 | 93.64 | 0.839 | 0.713 | 7.5 |
| | 50 | 94.48 | 0.898 | 0.647 | 6.80 |
| Site 2 | 10 | 90.44 | 0.344 | 1.431 | 16.03 |
| | 20 | 89.39 | 0.444 | 0.916 | 15.69 |
| | 30 | 88.08 | 0.214 | 1.567 | 17.56 |
| | 40 | 88.40 | 0.205 | 1.613 | 18.07 |
| | 50 | 87.02 | 0.227 | 1.593 | 17.85 |
| Site 3 | 10 | 86.80 | 0.519 | 1.572 | 13.38 |
| | 20 | 85.95 | 0.435 | 1.689 | 14.38 |
| | 30 | 86.68 | 0.511 | 1.606 | 13.67 |
| | 40 | 83.54 | 0.586 | 1.802 | 15.35 |
| | 50 | 82.92 | 0.330 | 1.989 | 16.94 |
| Site 4 | 10 | 92.39 | 0.637 | 1.073 | 9.32 |
| | 20 | 89.66 | 0.206 | 1.492 | 12.97 |
| | 30 | 91.83 | 0.621 | 1.007 | 8.75 |
| | 40 | 91.37 | 0.623 | 1.164 | 10.12 |
| | 50 | 90.67 | 0.539 | 1.220 | 10.61 |

**Table 4.** *Cont.*

| Serial Number | Minimum Number of Neighborhood Points | Accuracy (%) | $R^2$ | RMSE | rRMSE (%) |
|---|---|---|---|---|---|
| Site 5 | 10 | 89.68 | 0.691 | 1.513 | 14.02 |
| | 20 | 88.55 | 0.576 | 1.220 | 17.89 |
| | 30 | 90.03 | 0.728 | 1.398 | 12.96 |
| | 40 | 89.30 | 0.681 | 1.545 | 14.32 |
| | 50 | 88.65 | 0.634 | 0.586 | 14.70 |
| Site 6 | 10 | 94.44 | 0.865 | 0.702 | 7.26 |
| | 20 | 93.09 | 0.819 | 0.759 | 7.77 |
| | 30 | 93.87 | 0.832 | 0.725 | 7.50 |
| | 40 | 92.47 | 0.770 | 0.883 | 9.14 |
| | 50 | 92.78 | 0.808 | 0.784 | 8.11 |

Based on a minimum neighborhood point set to 10, denoising was performed with five standard deviation multiples, as shown in Table 5. Sites 3, 4, 5, and 6 exhibited the highest accuracy of fit for DBH at a standard deviation multiplier of 2, with accuracies of 91.05%, 92.63%, 92.12%, and 94.72%, respectively, corresponding to $R^2$ values of 0.645, 0.637, 0.740, and 0.872. The *RMSE* and *rRMSE* for the fitted and measured values of DBH for site 6 were the smallest, at 0.668 and 6.91%, respectively. On the other hand, sites 1 and 2 showed the highest accuracy of fitting DBH at a standard deviation multiplier of 1, with accuracies of 96.37% and 90.44%, respectively. The denser growth of Moso bamboo in sites 1 and 2 led to more compact and noisy point cloud data, where a standard deviation multiplier of 1 effectively removed noise and yielded higher-quality point cloud data. In contrast, sites 3, 4, 5, and 6 displayed sparse growth of Moso bamboo, with relatively fewer noise points in the point cloud data. Adjusting the standard deviation multiplier to 1 impacted the structure of the Moso bamboo point cloud itself, influencing the accuracy of DBH fit, while a higher standard deviation multiplier preserved more noise points, also affecting the fit of DBH.

**Table 5.** DBH fitting results after denoising with different standard deviation multiples.

| Serial Number | Standard Deviation Multiplier | Accuracy (%) | $R^2$ | RMSE | rRMSE (%) |
|---|---|---|---|---|---|
| Site 1 | 1 | 96.37 | 0.959 | 0.416 | 4.38 |
| | 2 | 94.06 | 0.896 | 0.728 | 7.66 |
| | 3 | 93.60 | 0.778 | 0.870 | 9.15 |
| | 4 | 94.20 | 0.215 | 0.761 | 8.00 |
| | 5 | 94.91 | 0.902 | 0.633 | 6.66 |
| Site 2 | 1 | 90.44 | 0.344 | 1.431 | 16.03 |
| | 2 | 89.58 | 0.411 | 1.357 | 15.20 |
| | 3 | 88.30 | 0.241 | 1.539 | 17.24 |
| | 4 | 88.06 | 0.282 | 1.492 | 16.71 |
| | 5 | 89.09 | 0.424 | 1.365 | 15.29 |
| Site 3 | 1 | 86.80 | 0.519 | 1.57 | 13.38 |
| | 2 | 91.05 | 0.645 | 1.157 | 9.85 |
| | 3 | 88.39 | 0.508 | 1.408 | 11.99 |
| | 4 | 87.89 | 0.567 | 1.480 | 12.60 |
| | 5 | 88.97 | 0.486 | 1.390 | 11.84 |
| Site 4 | 1 | 92.39 | 0.515 | 1.073 | 9.32 |
| | 2 | 92.63 | 0.637 | 1.071 | 9.31 |
| | 3 | 92.51 | 0.367 | 1.154 | 10.03 |
| | 4 | 92.49 | 0.449 | 1.159 | 10.08 |
| | 5 | 92.52 | 0.499 | 1.118 | 9.72 |

**Table 5.** *Cont.*

| Serial Number | Standard Deviation Multiplier | Accuracy (%) | $R^2$ | RMSE | rRMSE (%) |
|---|---|---|---|---|---|
| | 1 | 89.68 | 0.691 | 1.513 | 14.02 |
| | 2 | 92.12 | 0.740 | 1.316 | 12.20 |
| Site 5 | 3 | 89.70 | 0.578 | 1.710 | 15.85 |
| | 4 | 89.98 | 0.544 | 1.771 | 16.42 |
| | 5 | 89.21 | 0.583 | 1.737 | 16.11 |
| | 1 | 94.44 | 0.865 | 0.702 | 7.26 |
| | 2 | 94.72 | 0.872 | 0.668 | 6.91 |
| Site 6 | 3 | 94.36 | 0.857 | 0.731 | 7.56 |
| | 4 | 93.23 | 0.816 | 0.822 | 8.50 |
| | 5 | 94.10 | 0.868 | 0.680 | 7.03 |

### 3.3. DBH Extraction Results and Analysis

The results presented in Figure 9 are based on the optimal parameter fitted to the diameter of Moso bamboo chests. The correlations between the fitted and measured values of Moso bamboo diameter at each sample site were 0.959, 0.344, 0.654, 0.515, 0.740, and 0.872, respectively. Notably, site 1 exhibited the highest correlation between the fitted and measured values of diameter, with the lowest *RMSE* and *rRMSE* values of 0.416 and 4.38%, respectively. Following closely, site 6 showed an *RMSE* of 0.668 and *rRMSE* of 6.91%. Conversely, site 2 displayed the lowest correlation, resulting in the highest *RMSE* and *rRMSE* values of 1.431 and 16.03%.
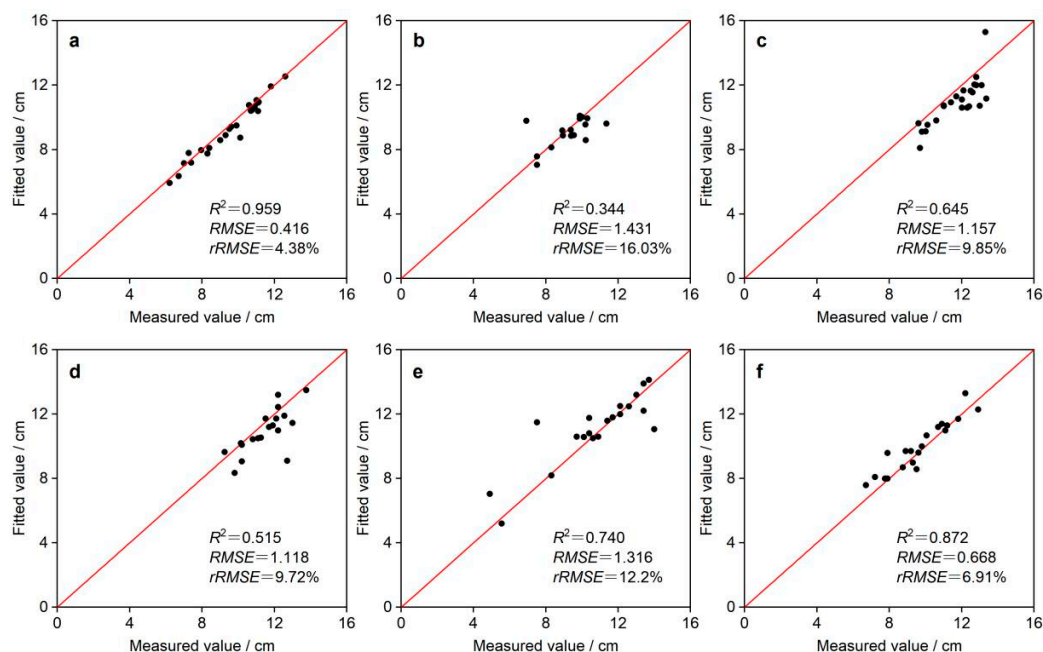


**Figure 9.** Regression analysis of fitted and measured values of bamboo DBH in the sample site. (**a–f**) represent site 1-6, respectively. Note: straight line represents $y = x$.

Site 1 exhibited a smaller slope with fewer overgrown shrubs shading the bamboo pole area, resulting in a higher-quality point cloud collection. In contrast, the discrepancy between the fitted and measured values of DBH for site 2 can be attributed to the presence of a greater variety of mixed shrubs in the understory. Additionally, the presence of intertwined and fallen Moso bamboo plants in site 2 may have led to inaccuracies in contour representation during single wood splitting, resulting in errors when fitting the DBH.

*3.4. Analysis of Errors*

In order to investigate the sources of error, eight Moso bamboo plants with significant discrepancies in the fitted values of DBH were chosen for analysis (Table 6).

**Table 6.** Error analysis table.

| Serial ID | Measured DBH (cm) | Fitted DBH (cm) |
|---|---|---|
| MZ02dm01 | 6.9 | 8.8 |
| MZ03dm04 | 13.4 | 11.2 |
| MZ03dm25 | 13.0 | 10.7 |
| MZ04dm10 | 12.7 | 9.1 |
| MZ04dm11 | 9.8 | 8.3 |
| MZ05dm03 | 7.5 | 11.5 |
| MZ05dm05 | 5.0 | 10.5 |
| MZ06dm12 | 7.9 | 9.7 |

The measured DBH of Moso bamboo MZ2dm01 was 6.9 cm, while the fitted DBH was 8.8 cm, indicating a difference of 1.9 cm between the measured and fitted values. This error was attributed to noisy point cloud data at 1.3 m, resulting in unclear contours (Figure 10a). Similarly, the measured DBH of Moso bamboo MD3dm04 was 13.4 cm, whereas the fitted DBH was 11.2 cm, showing a discrepancy of 2.2 cm. This discrepancy was due to excessive stray irradiation in the area, causing the laser light to be absorbed by branches and trunks, leading to inaccurate echo signals and an inability to accurately capture the profile of the single Moso bamboo plant (Figure 10b). Additionally, the measured DBH of Moso bamboo MD3dm25 was 13.0 cm, while the fitted DBH was 10.7 cm. The discrepancy in this case was caused by the close proximity of two Moso bamboo plants, resulting in misidentification. Subsequently, another Moso bamboo plant was manually refitted with a DBH of 11.5 cm, achieving an accuracy of 88.46% (Figure 10c). The measured DBH of Moso bamboo MD4dm10 was 12.7 cm, while the fitted DBH was 9.1 cm. Unfortunately, the point cloud data for this specimen were significantly missing (Figure 10d). In the case of MD4dm11, the measured DBH was 9.8 cm, with a fitted DBH of 8.3 cm. Similar to MD4dm10, the point cloud data were also missing (Figure 10e). Moving on to Moso bamboo MD5dm03, the measured diameter was 7.5 cm, but the fitted diameter was 11.5 cm, resulting in a large fitted value. The outline of the Moso bamboo in the point cloud appeared fuzzy and overlapping, possibly due to rapid scanner movements causing multiple scans of the same area, leading to an abundance of repetitive data points that impacted accuracy (Figure 10f). Continuing with MD5dm05, the measured DBH was 5.0 cm, while the fitted DBH was 10.6 cm, showing a large fitted value caused by fuzzy overlap in the point cloud data at 1.3 m (Figure 10g). Lastly, for Moso bamboo MD6dm12, the measured DBH was 7.9 cm, with a fitted DBH of 9.7 cm. The data indicated a significant break at 1.3 m, likely resulting from a splicing error during the normalization process due to the steep slope of the sample site (Figure 10h).

The challenges in accurately fitting the Moso bamboo DBH using handheld LiDAR data can be attributed to two main factors. Firstly, the dense forest conditions in the scanned sample plots, characterized by numerous low shrubs in the understory, lead to laser absorption and inadequate return, resulting in a point cloud with lower density and reduced quality. This hindered the precise representation of Moso bamboo outlines post-data processing. Secondly, the presence of tilted and overlapping Moso bamboo in some areas caused ambiguity in the point cloud data, further complicating accurate outline depiction. Additionally, in sample plots with steep slopes, maintaining consistent scanning speed and smooth travel paths proved challenging, impacting point cloud alignment and leading to stitching errors. Consequently, the accurate representation of Moso bamboo outlines became compromised.
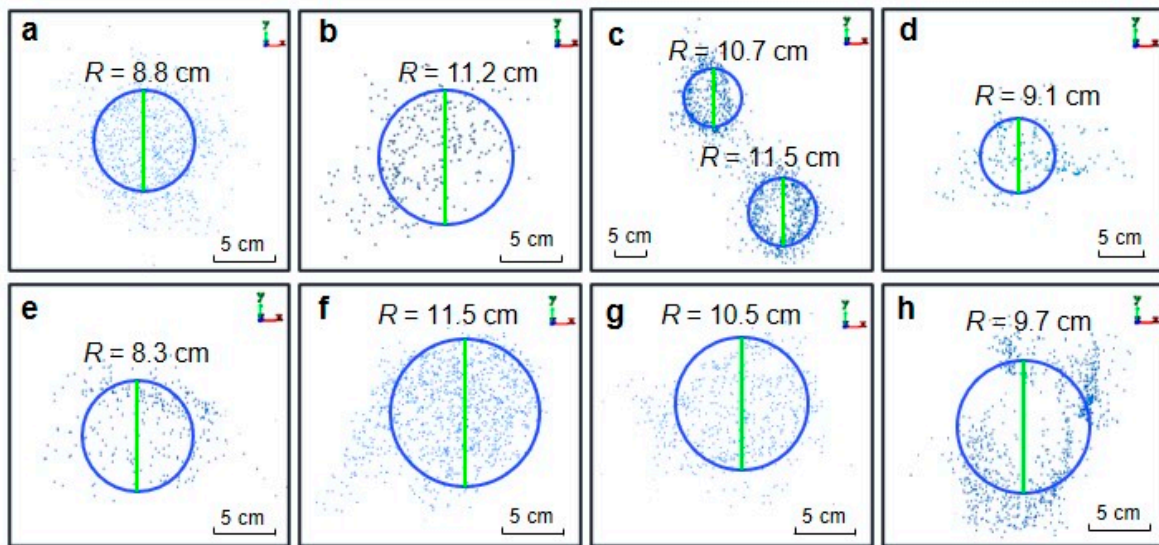
**Figure 10.** Error analysis for DBH fitting. (**a**–**h**) represent eight individual Moso bamboo with the largest DBH fitting error.

After excluding points with large errors, the results of the fitted and measured values of DBH are presented in Figure 11 and Table 7. The extraction accuracy of DBH for sample sites 2–6 generally improved, with an increase in $R^2$ and a decrease in both *RMSE* and *rRMSE*. Overall, after removing points with large errors, all evaluation parameters were significantly optimized.



**Figure 11.** Regression analysis chart between the fitted and measured values of corrected DBH. (**a**–**f**) represent site 1-6, respectively. Note: straight line represents *y* = *x*.

**Table 7.** Precision evaluation results before and after removing points with significant errors.

| Sample Site | Pre-Deletion | | | | Post-Deletion | | | |
|---|---|---|---|---|---|---|---|---|
| | Accuracy (%) | $R^2$ | *RMSE* | *rRMSE* (%) | Accuracy (%) | $R^2$ | *RMSE* | *rRMSE* (%) |
| Site 1 | 96.37 | 0.959 | 0.416 | 4.38 | 96.37 | 0.959 | 0.416 | 4.38 |
| Site 2 | 90.44 | 0.344 | 1.431 | 16.03 | 95.42 | 0.672 | 0.694 | 7.37 |
| Site 3 | 91.05 | 0.645 | 1.157 | 9.85 | 94.24 | 0.732 | 0.915 | 7.84 |
| Site 4 | 92.63 | 0.637 | 1.071 | 9.31 | 95.48 | 0.729 | 0.714 | 6.19 |
| Site 5 | 92.12 | 0.740 | 1.316 | 12.20 | 96.71 | 0.931 | 0.565 | 5.08 |
| Site 6 | 94.72 | 0.872 | 0.668 | 6.91 | 95.60 | 0.903 | 0.564 | 5.78 |

## 4. Discussions

This study utilized a handheld LiDAR device to gather point cloud data from samples of Moso bamboo. The data underwent denoising, ground point classification, normalization, and single-wood segmentation operations. Subsequently, the single Moso bamboo DBH was extracted using the least-squares circle fitting method and compared with the measured DBH for accuracy evaluation.

Compared to terrestrial laser scanning and backpack laser scanning, handheld LiDAR is capable of scanning more complex forest environments. Terrestrial laser scanning, when scanning dense vegetation, often requires setting up multiple sites in different locations and spending a significant amount of time on data processing. On the other hand, backpack laser scans from a higher height than the scanning personnel, making it susceptible to damage from branches and leaves at lower branch heights or complex forest conditions. This can lead to sensor damage and a decrease in point cloud quality due to obstruction from branches and leaves. In contrast, the handheld LiDAR scanner is compact, lightweight, easy to carry, and simple to operate. It enables the quick collection of point cloud data in complex secondary forests, resulting in higher measurement efficiency.

The utilization of handheld LiDAR scanners for arborimetric measurements is a significant advancement in modern forestry and ecological research. This study has demonstrated the effectiveness of using handheld LiDAR scanners to measure the DBH of Moso bamboo. By utilizing point cloud data from these portable devices, additional parameters such as tree height, LAI, and canopy spread can be extracted. These variables play a crucial role in modeling tree growth patterns, understanding vertical canopy structure, and improving estimates of forest carbon sequestration—a critical aspect of global change ecology. Moreover, detailed characterizations of individual trees aid in creating accurate forest biomass maps and enhance our ability to monitor ecosystem services like carbon storage and habitat suitability. Apart from ecological applications, the high-resolution data obtained from handheld LiDAR systems can also support precision forestry initiatives, capturing the intricacies and diversity of forest environments. Therefore, future research should focus on exploring the potential of handheld LiDAR scanners in various dendrometric applications, including evaluating their suitability for measuring unconventional parameters, validating their accuracy against traditional methods, and incorporating them into innovative ecological models that simulate forest responses to environmental stressors.

In this study, only five parameter intervals were selected through the experimental screening of suitable denoising parameters. Subsequent processing can continue to further refine these parameters in order to improve the accuracy of DBH extraction. Precision forestry demands high accuracy in parameters such as single Moso bamboo identification and diameter extraction. The next step could involve attempting to fuse airborne and handheld LiDAR point cloud data to obtain higher-quality and more comprehensive point cloud data. This could pave the way for further research on parameters such as Moso bamboo tree height, bamboo age, biomass, and other related factors.

## 5. Conclusions

This research utilized handheld LiDAR technology to capture point cloud data of Moso bamboo forests in Taipinghu and Wushi Township, Huangshan City. This study conducted DBH fitting post-denoising using various parameters, assessed the accuracy, and examined the errors of the fitted values. The findings indicated a 93% accuracy in identifying Moso bamboo with a handheld LiDAR scanner and achieved an average DBH fitting accuracy of 95.64% after eliminating points with significant errors. The mean error was ±1.8 cm. Notably, setting the number of neighboring points to 10 resulted in the highest fitting accuracy for Moso bamboo diameter. This study observed varying outcomes in the extraction of samples based on different stand densities, suggesting an optimal threshold of 1 for the standard deviation multiplier in dense Moso bamboo sample sites and 2 for sparse Moso bamboo sample sites. Additionally, forest condition and slope were identified as key factors influencing the error in fitting DBH to handheld LiDAR data. Issues such as shrubs obstructing the laser, intertwined bamboo growth affecting point cloud quality, and errors in data from samples with steep slopes were noted.

**Author Contributions:** Conceptualization, L.L., L.W. and N.L.; Methodology, L.L. and L.W.; Software, L.W. and S.Z.; Validation, L.W., S.Z. and Z.W.; Data curation, L.W., Z.W. and M.D.; Formal analysis, L.W., S.Z. and Z.W.; Funding acquisition, L.L. and M.D.; Investigation, L.L., L.W., N.L., S.Z., Z.W., M.D. and Y.C.; Visualization, L.L., L.W. and N.L.; Writing—original draft preparation, L.L., L.W. and N.L.; Writing—review and editing, L.L., L.W., N.L., S.Z., Z.W. and M.D.; Supervision, N.L. All authors have read and agreed to the published version of the manuscript.

**Data Availability Statement:** The raw data supporting the conclusions of this article will be made available by the authors on request.

**Conflicts of Interest:** Author Yuyun Chen is employed by the company Shanghai Ubiquitous Navigation Technology Co., Ltd. The remaining authors declare that this research was conducted in the absence of any commercial or financial relationships that could be construed as a potential conflict of interest. The Company Shanghai Ubiquitous Navigation Technology Co., Ltd. had no role in the design of the study; in the collection, analyses, or interpretation of data; in the writing of the manuscript; or in the decision to publish the results.

## References

1. Liu, C.; Zhou, Y.; Qin, H.; Liang, C.; Shao, S.; Fuhrmann, J.J.; Chen, J.; Xu, Q. Moso bamboo invasion has contrasting effects on soil bacterial and fungal abundances, co-occurrence networks and their associations with enzyme activities in three broadleaved forests across subtropical China. *For. Ecol. Manag.* **2021**, *498*, 119549. [CrossRef]
2. Li, L.; Zhu, H.; Wu, T.; Wei, L.; Li, N. New landscape-perspective exploration of Moso bamboo forests under on/off-year phenomena and human activities. *Front. For. Glob. Change* **2023**, *6*, 1204329. [CrossRef]
3. Zheng, Y.; Fan, S.; Guan, F.; Xia, W.; Wang, S.; Xiao, X. Strip Clearcutting Drives Vegetation Diversity and Composition in the Moso Bamboo Forests. *For. Sci.* **2022**, *68*, 27–36. [CrossRef]
4. Yuen, J.Q.; Fung, T.; Ziegler, A.D. Carbon stocks in bamboo ecosystems worldwide: Estimates and uncertainties. *For. Ecol. Manag.* **2017**, *393*, 113–138. [CrossRef]
5. Scurlock, J.M.O.; Dayton, D.C.; Hames, B. Bamboo: An overlooked biomass resource? *Biomass Bioenergy* **2000**, *19*, 229–244. [CrossRef]
6. Li, L. Phenology Examination, Classification and Aboveground Biomass Estimation of Moso Bamboo Forests Using Time Series Remote Sensing Data. Ph.D. Thesis, Zhejiang A&F University, Hangzhou, China, 2020.
7. Zhou, G.; Meng, C.; Jiang, P.; Xu, Q. Review of Carbon Fixation in Bamboo Forests in China. *Bot. Rev.* **2011**, *77*, 262–270. [CrossRef]

8. Shendryk, I.; Broich, M.; Tulbure, M.G.; Alexandrov, S.V. Bottom-up delineation of individual trees from full-waveform airborne laser scans in a structurally complex eucalypt forest. *Remote Sens. Environ.* **2016**, *173*, 69–83. [CrossRef]

9. Li, L.; Li, N.; Lu, D.; Chen, Y. Mapping Moso bamboo forest and its on-year and off-year distribution in a subtropical region using time-series Sentinel-2 and Landsat 8 data. *Remote Sens. Environ.* **2019**, *231*, 111265. [CrossRef]

10. Proudman, A.; Ramezani, M.; Digumarti, S.T.; Chebrolu, N.; Fallon, M. Towards real-time forest inventory using handheld LiDAR. *Robot. Auton. Syst.* **2022**, *157*, 104240. [CrossRef]

11. Zhao, L.; Zhang, X.; Sun, H. Application of LiDAR data to forest parameters estimation. *World For. Res.* **2010**, *23*, 61–64.

12. Pham, D.D.; Suh, Y.S. Remote length measurement system using a single point laser distance sensor and an inertial measurement unit. *Comput. Stand. Interfaces* **2017**, *50*, 153–159. [CrossRef]

13. Polewski, P.; Yao, W.; Cao, L.; Gao, S. Marker-free coregistration of UAV and backpack LiDAR point clouds in forested areas. *ISPRS J. Photogramm. Remote Sens.* **2019**, *147*, 307–318. [CrossRef]

14. Cai, S.; Xin, Y.; Duan-Mu, J. Extraction of DBH from filtering out low intensity point cloud by backpack laser scanning. *For. Eng.* **2021**, *37*, 12–19.

15. Brolly, G.; Kiraly, G.; Lehtomaki, M.; Liang, X. Voxel-based automatic tree detection and parameter retrieval from terrestrial laser scans for plot-wise forest inventory. *Remote Sens.* **2021**, *13*, 542. [CrossRef]

16. Cai, Y.; Xu, W.; Liang, D.; Deng, S.; Li, C. Distinguishing *Phyllostachys edulis* age based on laser scanning intensity. *Chin. J. Lasers* **2018**, *45*, 272–280.

17. Li, L.; Sun, Y.; Wan, F.; Xu, X.; Huang, X. Research on canopy height inversion of Moso bamboo forests on Ta-pieh Mountains based on LiDAR. *J. Bamboo Res.* **2022**, *41*, 10–16.

18. Huang, L.; Guan, F. Retrieving parameters of individual Moso bamboo using terrestrial laser scanning data. *J. Northeast For. Univ.* **2021**, *49*, 67–70, 114.

19. Jiang, R.; Lin, J.; Li, T. Refined Aboveground Biomass Estimation of Moso Bamboo Forest Using Culm Lengths Extracted from TLS Point Cloud. *Remote Sens.* **2022**, *14*, 5537. [CrossRef]

20. Yang, B.; Liang, F.; Huang, R. Progress, challenges and perspectives of 3D LiDAR point cloud processing. *Acta Geod. Cartogr. Sin.* **2017**, *46*, 1509–1516.

21. Lu, D.; Zou, G. Comparative research on denoising algorithms of 3D laser point cloud. *Bull. Surv. Mapp.* **2019**, *S2*, 102–105.

22. Zhao, X.; Guo, Q.; Su, Y.; Xue, B. Improved progressive TIN densification filtering algorithm for airborne LiDAR data in forested areas. *ISPRS J. Photogramm. Remote Sens.* **2016**, *117*, 79–91. [CrossRef]

23. Lee, H.; Slatton, K.C.; Roth, B.E.; Cropper, W.P. Adaptive clustering of airborne LiDAR data to segment individual tree crowns in managed pine forests. *Int. J. Remote Sens.* **2010**, *31*, 117–139. [CrossRef]

24. Li, W.; Guo, Q.; Jakubowski, M.K.; Kelly, M. A New Method for Segmenting Individual Trees from the Lidar Point Cloud. *Photogramm. Eng. Remote Sens.* **2012**, *78*, 75–84. [CrossRef]

25. Liu, C.; Xing, Y.; Duanmu, J.; Tian, X. Evaluating different methods for estimating diameter at breast height from terrestrial laser scanning. *Remote Sens.* **2018**, *10*, 513. [CrossRef]

26. Haris, B.; Jasmin, V.; Walter, B.; De Cubber, S.; Bruno, S. Fast Statistical Outlier Removal Based Method for Large 3D Point Clouds of Outdoor Environments. *IFAC-PapersOnLine* **2018**, *51*, 348–353.